
EXTENDING MULTI-MODAL CONTRASTIVE REPRESENTATIONS

Zehan Wang*
Zhejiang University

Ziang Zhang*
Zhejiang University

Luping Liu
Zhejiang University

Yang Zhao
ByteDance

Haifeng Huang
Zhejiang University

Tao Jin
Zhejiang University

Zhou Zhao
Zhejiang University

ABSTRACT

Multi-modal contrastive representation (MCR) of more than three modalities is critical in multi-modal learning. Although recent methods showcase impressive achievements, the high dependence on large-scale, high-quality paired data and the expensive training costs limit their further development. Inspired by recent C-MCR, this paper proposes **Extending Multimodal Contrastive Representation (Ex-MCR)**, a training-efficient and paired-data-free method to flexibly learn unified contrastive representation space for more than three modalities by integrating the knowledge of existing MCR spaces. Specifically, Ex-MCR aligns multiple existing MCRs into the same based MCR, which can effectively preserve the original semantic alignment of the based MCR. Besides, we comprehensively enhance the entire learning pipeline for aligning MCR spaces from the perspectives of training data, architecture, and learning objectives. With the preserved original modality alignment and the enhanced space alignment, Ex-MCR shows superior representation learning performance and excellent modality extensibility. To demonstrate the effectiveness of Ex-MCR, we align the MCR spaces of CLAP (audio-text) and ULIP (3D-vision) into the CLIP (vision-text), leveraging the overlapping text and image modality, respectively. Remarkably, without using any paired data, Ex-MCR learns a 3D-image-text-audio unified contrastive representation, and it achieves state-of-the-art performance on audio-visual, 3D-image, audio-text, visual-text retrieval, and 3D object classification tasks. More importantly, extensive qualitative results further demonstrate the emergent semantic alignment between the extended modalities (e.g., audio and 3D), which highlights the great potential of modality extensibility. Our code is available at <https://github.com/MCR-PEFT/Ex-MCR>.

1 INTRODUCTION

Multi-modal Contrastive Representation (MCR) learning endeavors to align inputs from diverse modalities within a shared representation space. Recently, the high-quality contrastive representations of more than three modalities attract increasing attention (Girdhar et al., 2023; Guzhov et al., 2022; Xue et al., 2023a;b; Liu et al., 2023b; Hegde et al., 2023; Guo et al., 2023), and play a fundamental role in many application scenarios of multi-modal understanding (Su et al., 2023; Zhang et al., 2023; Zhao et al., 2023; Wang et al., 2023a; Han et al., 2023) and generation (Tang et al., 2023; Liu et al., 2023a; Ramesh et al., 2022; Rombach et al., 2022; Gafni et al., 2022; Huang et al., 2023a). Despite the achievements of multi-modal contrastive learning, its broader and more flexible application is still constrained by the high dependence on large-scale, high-quality paired data and extremely costly training resources.

Recently, Wang et al. (2023b) introduces a novel training-efficient method, called C-MCR, for learning contrastive representations between modalities that lack paired data by mining knowledge from existing MCR spaces. It connects two pre-trained MCRs onto a new shared space via overlapping modalities. Since the modalities of each MCR are intrinsically aligned, the connection learned

*Equal contribution. Contact: {wangzehan01, ziangzhang}@zju.edu.cn

from overlapping modalities can also be transferred to non-overlapping modalities. Experimentally, without using image-audio and 3D-text data pairs, C-MCR demonstrates advanced performance in image-audio and 3D-text downstream tasks.

Despite the remarkable flexibility and performance of C-MCR, its broader applications are hindered by a critical limitation: C-MCR mainly focuses on learning a new space for the two non-overlapping modalities, while the original modality alignments in powerful pre-trained MCRs are forgotten. As a result of the decline of original alignment, C-MCR faces challenges in concurrently establishing connections among three or more MCRs. Therefore, C-MCR can not be used to flexibly learn a shared contrastive representation space for more than three modalities.

This paper introduces **Extending Multi-modal Contrastive Representations (Ex-MCR)**, a novel training-efficient and paired-data-free unified representation learning method with excellent modality extensibility. Ex-MCR better preserves the alignment within the original pre-trained MCR space and enhances the overall learning pipeline to align different MCR spaces more robustly. Specifically, the two important designs of Ex-MCR are discussed in detail below:

Firstly, we extend one MCR space (called leaf-MCR) into another fixed MCR space (called base-MCR) rather than connecting two MCR spaces to a new space. Such a simple yet effective approach maximizes the preservation of modality alignment within the base MCR, demonstrating great potential for integrating multiple MCRs.

Secondly, we enhance the whole learning process to promote stronger alignment across different MCRs. Specifically: 1) From the training data perspective, we extract various modality-centric pseudo data pairs, aiming to alleviate the semantic bias of pseudo pairs in Wang et al. (2023b) and reflect MCR space more comprehensively. 2) From the architecture perspective, we propose a decoupled projector, which reduces interference among different optimization objectives. We further find that a simple linear mapping is more effective for learning to eliminate modality gaps within MCRs. 3) From the learning objective perspective, we employ a dense contrastive loss on pseudo-pairs between all possible modalities pairs, further enhancing the learned alignment’s stability.

Utilizing Ex-MCR, we can flexibly align multiple pre-trained leaf-MCR spaces onto a common base-MCR space without any paired data and with exceptionally low training costs. To evaluate the effectiveness of our Ex-MCR, we try to extend the ULIP (3D-image) and CLAP (audio-text) onto CLIP (image-text) via the overlapping image and text modality, respectively, which derive unified and high-quality audio-image-text-3D representations. Without using any paired data, Ex-MCR attains state-of-the-art performance results across various zero-shot tasks, including audio-visual, 3D-image, audio-text, visual-text retrieval, and 3D object classification. More importantly, semantic alignment is also observed between extended modalities (e.g., audio-3D), which highlights the potential of Ex-MCR in modality extensibility.

Our contributions can be summarized as three-fold:

- (1) We propose **Extending Multi-modal Contrastive Representations (Ex-MCR)**, a novel a training-efficient and paired-data-free representation learning method for more than three modalities.
- (2) We comprehensively enhance the entire learning pipeline for aligning MCR spaces from the perspectives of training data, architecture, and learning objectives. These novel designs offer valuable insights about effectively integrating knowledge within existing MCRs.
- (3) We obtain high-quality unified audio-image-text-3D representations using Ex-MCR, which exhibits advanced performance on a series of tasks and excellent modality scalability. Besides, we also conduct detailed ablation studies to verify the effectiveness of each proposed component.

2 RELATED WORKS

2.1 MULTI-MODAL CONTRASTIVE REPRESENTATIONS

Multi-modal Contrastive Representations (MCR) learning aims to acquire semantically aligned cross-modal representations by pretraining the model on large-scale paired data. These aligned representations play a pivotal role in downstream comprehension and generation tasks. Inspired by the success of CLIP (Radford et al., 2021), many works try to learning contrastive representa-

tions for two modalities (Radford et al., 2021; Li et al., 2022; 2021; Gan et al., 2022; Xu et al., 2021). CLIP (Radford et al., 2021) and ALIGN (Jia et al., 2021) learn shared vision-text representations from million-level image-text pairs. CLAP (Elizalde et al., 2023; Wu et al., 2023) learns the audio-text representation, and CAV-MAE (Gong et al., 2022) focus on acquiring shared audio-visual feature space. C-MCR (Wang et al., 2023b) focuses on learning new representation space by connecting the pre-trained spaces through overlapping modality.

Apart from aligning two modalities, shared representations for more than three modalities attract increasing attention. AudioCLIP (Guzhov et al., 2022) and WAV2CLIP (Wu et al., 2022) train an audio encoder aligned with CLIP using audio-text-image triplets data. ULIP (Xue et al., 2023a;b) and openshape (Liu et al., 2023b) construct 3D-image-text triplets data through rendering 3D mesh into 2D images and captioning images for textual description, thereby learning a corresponding 3D encoder for image-text MCR space. Furthermore, Imagebind (Han et al., 2023) exclusively utilizes data pairs between various modalities and images to expand CLIP with multiple modal alignment encoders.

However, these methods heavily rely on large-scale, high-quality paired data collected from the internet or generated automatically and exceptionally high computational resources. Due to the lack of high-quality paired data for more modal combinations, such as audio-visual and text-3D, the extensibility of representation learning is notably constrained. Furthermore, the exceedingly high computational costs also diminish the flexibility of MCR learning.

2.2 AUDIO-VISUAL AND 3D-TEXT LEARNING

Audio-vision and 3D-text learning have significant applications in multi-modal recognition (Gemmeke et al., 2017; Chen et al., 2020b; Chang et al., 2015; Dai et al., 2017), localization (Chen et al., 2020a; Achlioptas et al., 2020; Zhao et al., 2021; 2018; Mo & Morgado, 2022; Chen et al., 2021), question-answer (Wang et al., 2023a; Zhao et al., 2023; Azuma et al., 2022; Lin et al., 2023b), and generation (Ruan et al., 2023; Poole et al., 2022; Lin et al., 2023a). They also play important roles in robot-related tasks such as human-machine interaction and synthetic information obtaining in complex environments (Peng et al., 2023; Huang et al., 2023b).

However, audio-visual datasets (Gemmeke et al., 2017; Chen et al., 2020b) often suffer from substantial noise due to soundless objects and invisible sounds. Additionally, paired 3D-text data (Chang et al., 2015) is scarce and expensive to collect. The scarcity of large-scale datasets hampers the further advancement of 3D-text and audio-vision contrastive representations. Previous methods, such as AudioCLIP (Guzhov et al., 2022) and ULIP (Xue et al., 2023a;b), mainly focus on automatically collecting or generating more paired data, but they are still limited by the relatively low quality of the training datasets. Our approach overcomes the reliance on paired data, achieving superior performance in audio-vision and 3D-text retrieval without using any audio-vision or 3D-text data.

3 EXTENDING MULTI-MODAL CONTRASTIVE LEARNING

3.1 EXTENDING RATHER THAN CONNECTING

Given two pre-trained MCR spaces on modalities $(\mathcal{A}, \mathcal{B})$ and $(\mathcal{B}, \mathcal{C})$, C-MCR (Wang et al., 2023b) employs two projectors to map them into a new shared space, where the alignment of different MCRs can be learned from overlapping modality \mathcal{B} . Since each pre-trained MCR intrinsically contains the alignment of $(\mathcal{A}, \mathcal{B})$ and $(\mathcal{B}, \mathcal{C})$, the alignment learned from overlapping modality theoretically can be transferred to the non-overlapping modalities. Specifically, the embeddings from overlapping modality \mathcal{B} but different MCR are aligned via an InfoNCE loss in the new space. Besides, C-MCR retrieves pseudo $(\mathcal{A}, \mathcal{C})$ pairs using the same data of \mathcal{B} and these pseudo-pairs are also aligned for a more comprehensive inter-MCR alignment. Moreover, C-MCR employs L2 loss between the embeddings from the same MCR space but different modalities to close the modality gap (Liang et al., 2022), significantly enhancing the transferability of learned inter-MCR alignment. C-MCR has remarkable flexibility and versatility since learning a novel C-MCR space requires two learnable MLPs and unpaired unimodal data.

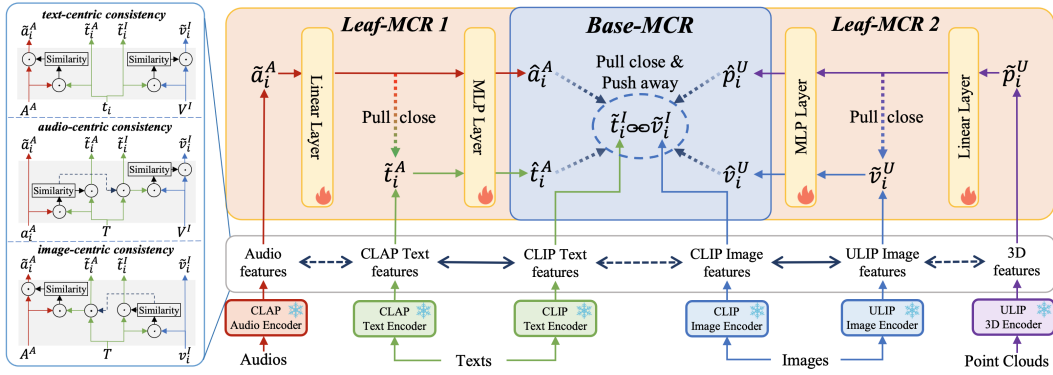


Figure 1: **The pipeline of extending leaf-MCRs (CLAP, ULIP) to base-MCR (CLIP).** For aligning CLAP to CLIP, we take audio, text, and image as input and encode them individually with frozen encoders in CLAP and CLIP. As shown in the left subfigure, we iteratively take the three kinds of modalities as query to generate pseudo-pairs. For aligning ULIP to CLIP, we take a symmetrical approach. When inferencing, audio and 3D inputs are inputted to the CLAP audio encoder and ULIP 3D encoder, then mapped into the CLIP MCR space via the corresponding projectors. Texts and images are encoded by the CLIP text encoder and image encoder.

However, C-MCR mainly focuses on learning a new space for the two non-overlapping modalities (\mathcal{A} , \mathcal{C}), while the original modality alignment (\mathcal{A} , \mathcal{B}) and (\mathcal{B} , \mathcal{C}) in powerful pre-trained MCRs are forgotten. As a result of the decline of original alignment, C-MCR faces challenges in concurrently establishing connections among three or more MCRs. Therefore, C-MCR can not be used to flexibly learn a shared contrastive representation space for more than three modalities.

To achieve a training-efficient and paired-data-free unified contrastive representation method, we propose to extend one MCR to another rather than connect the two MCRs to a new space. Considering the two MCR spaces on modalities (\mathcal{A} , \mathcal{B}) and (\mathcal{B} , \mathcal{C}), Ex-MCR chooses one as the base-MCR (\mathcal{A} , \mathcal{B}), and the other as the leaf-MCR (\mathcal{B} , \mathcal{C}). In the ‘‘Extended’’ scheme, the base-MCR space is frozen, and we only train one projector to map leaf-MCR to base-MCR utilizing the overlapping modalities \mathcal{B} . Specifically, we employ the native pairs of \mathcal{B} and pseudo pairs generated by \mathcal{B} to learn aligning leaf-MCR to base-MCR via InfoNCE loss. Simultaneously, we employ the L2 loss to bridge the modality gap between (\mathcal{B} , \mathcal{C}) modalities of leaf-MCR, thereby facilitating more transferable alignments between the MCR spaces.

In contrast to C-MCR, Ex-MCR can conveniently expand more MCR spaces. Benefiting from efficient training and no need to pair data, we can flexibly align multiple leaf-MCR spaces to the same base-MCR space. In addition to explicitly establishing modality alignment within leaf-MCR and base-MCR, semantic alignment also emerges among extended modalities. Ex-MCR leverages the pivotal role of the base-MCR, employing it as a bridge for achieving semantic alignment among modalities in multiple leaf-MCR spaces.

3.2 ENHANCING ALIGNMENT LEARNING PIPELINE

Before delving into the details of our learning pipeline, we first clarify the necessary symbols and notations. We align the audio-text space of CLAP and the 3D-image space of ULIP (leaf-MCRs) to the image-text space of CLIP (base-MCR). The unimodal inputs of audio, text, image, and 3D point cloud are denoted as A , T , V , and P , respectively. The audio features, extracted from the CLAP audio encoder, are denoted as $\mathbf{A}^A = \{\mathbf{a}_1^A, \mathbf{a}_2^A, \dots, \mathbf{a}_N^A\}$. Similarly, employing the encoders of CLAP, CLIP, and ULIP, we can extract corresponding sets of features \mathbf{T}^A , \mathbf{T}^I , \mathbf{V}^I , \mathbf{V}^U , and \mathbf{P}^U , where the superscripts A , I , and U represent encoding by CLAP, CLIP, and ULIP, respectively.

In Ex-MCR, freezing base-MCR allows us to preserve the original alignment of base-MCR but also implies that the modality gap within base-MCR remains preserved. Consequently, it becomes necessary to map the features of leaf-MCR to more suitable positions within the base-MCR space. To this end, we enhance the entire alignment learning pipeline from the perspectives of training

data, architecture, and learning objectives. This enhanced learning pipeline effectively improves alignment’s comprehensiveness, stability, and accuracy. Below, we sequentially introduce the design behind each perspective and corresponding motivations.

3.2.1 VARIOUS MODALITY-CENTRIC DATA

C-MCR employs data from overlapping modalities to aggregate semantic consistent embedding of non-overlapping modalities, thereby creating pseudo-pairs. This approach prompts a more comprehensive alignment. However, such a single modality-centric data is often biased and noisy. Taking CLIP and CLAP as an example, text encoders in CLIP and CLAP may introduce individual biases when encoding the same text, and texts can not describe the entire diverse visual or audio world. Therefore, the semantics of the text-centric pseudo-audio-image pairs are limited by the expressive power of text modality. The text-centric generated audio and image embeddings struggle to capture the entire audio and image representation space distribution.

To tackle the problem of limited and biased training data, we propose aggregating various modality-centric data. As depicted in the left sub-figure of Fig. 1, we no longer only take the overlapping modality as the query. Instead, all modalities in the two MCR spaces are iteratively employed as queries to aggregate corresponding semantically consistent embeddings. Take aligning CLAP to CLIP as an example; the overlapping modality-centric (e.g., text-centric) consistent embeddings can be aggregated as follows:

$$\begin{aligned}\tilde{\mathbf{t}}_i^A &= \mathbf{t}_i^A; & \tilde{\mathbf{a}}_i^A &= \text{softmax}((\tilde{\mathbf{t}}_i^A \cdot \mathbf{T}^A)/\tau_1) \cdot (\mathbf{T}^A)^T; \\ \tilde{\mathbf{t}}_i^I &= \mathbf{t}_i^I; & \tilde{\mathbf{v}}_i^I &= \text{softmax}((\tilde{\mathbf{t}}_i^I \cdot \mathbf{V}^I)/\tau_1) \cdot (\mathbf{V}^I)^T\end{aligned}\quad (1)$$

Where the τ_1 is the temperature parameter of softmax. The $\tilde{\mathbf{t}}_i^A$ and $\tilde{\mathbf{t}}_i^I$ are derived from the same text data, and their semantics are natively consistent. Benefiting from the modality semantic alignment within each MCR, the generated $\tilde{\mathbf{a}}_i^A$ and $\tilde{\mathbf{v}}_i^I$ are also semantically relevant to the $\tilde{\mathbf{t}}_i^A$ and $\tilde{\mathbf{t}}_i^I$.

To capture the representation space of non-overlapping modality more comprehensively, we further introduce non-overlapping modality-centric (e.g., audio-centric or image-centric) data. This process (take audio-centric as an example) can be expressed as:

$$\begin{aligned}\tilde{\mathbf{a}}_i^A &= \mathbf{a}_i^A; & \tilde{\mathbf{t}}_i^A &= \text{softmax}((\mathbf{a}_i^A \cdot \mathbf{T}^A)/\tau_1) \cdot (\mathbf{T}^A)^T \\ \tilde{\mathbf{t}}_i^I &= \text{softmax}((\mathbf{a}_i^A \cdot \mathbf{T}^A)/\tau_1) \cdot (\mathbf{T}^I)^T; & \tilde{\mathbf{v}}_i^I &= \text{softmax}((\tilde{\mathbf{t}}_i^I \cdot \mathbf{V}^I)/\tau_1) \cdot (\mathbf{V}^I)^T\end{aligned}\quad (2)$$

Since the embeddings of \mathbf{T}^A and \mathbf{T}^I of overlapping modality are one-to-one matched, the similarity weights between \mathbf{a}_i^A and \mathbf{T}^A can be naturally transferred for aggregating embeddings of \mathbf{T}^I . These pseudo-embedding pairs derived from audio can better reflect the representation space of audio. Based on the aforementioned formulas, when extending CLAP to CLIP, we can acquire three kinds (e.g., audio-centric, text-centric and image-centric) of semantically consistent embeddings $\{\tilde{\mathbf{a}}_i^A, \tilde{\mathbf{t}}_i^A, \tilde{\mathbf{t}}_i^I, \tilde{\mathbf{v}}_i^I\}$. These three kinds of data are combined and shuffled for training.

3.2.2 DECOUPLED PROJECTOR

The main network structure of Ex-MCR is a projector, and it serves two purposes: 1) Learning the intra-MCR alignment to close the modality gaps within leaf-MCR and prompt more stable alignment between MCRs. 2) Learning the inter-MCR alignment for extending leaf-MCR to base-MCR. Considering these two different purposes, we propose a decoupled projector to alleviate the potential conflict between distinct optimization objectives while exploring a more reasonable mapping layer design for these two purposes. As shown in Fig. 1, the projector is decoupled into a linear layer $f_l(\cdot)$ for intra-MCR alignment and a multi-layer perceptron (MLP) layer $f_m(\cdot)$ for inter-MCR alignment. For the example of extending CLAP to CLIP, we first use f_l to align $\tilde{\mathbf{a}}_i^A$ to $\tilde{\mathbf{t}}_i^A$ via L2 loss, which can be formulated as:

$$L_{intra} = \frac{1}{2} \frac{1}{B} \sum_{i=1}^B \|f_l(\tilde{\mathbf{a}}_i^A) - \tilde{\mathbf{t}}_i^A\|_2 \quad (3)$$

With this intra-MCR alignment loss, $f_l(\cdot)$ learns the mapping between audio subspace and text subspace within the CLAP, thereby effectively closing the modality gap. Since the subspaces of different modalities in MCR space are actually very similar, linear mapping is enough to bridge the

modality gap. Moreover, our experiments even found that activation layers have a negative effect on bridging the modality gap.

After bridging the modality gap, the shared $f_m(\cdot)$ are employed to map both audio and text embeddings of CLAP space to the CLIP space, which can be expressed as:

$$\hat{\mathbf{a}}_i^A = f_m(f_l(\tilde{\mathbf{a}}_i^A)); \quad \hat{\mathbf{t}}_i^A = f_m(\mathbf{t}_i^A) \quad (4)$$

3.2.3 DENSE ALIGNMENT OBJECTIVE

Since the modality gap within base-MCR is retained, a more robust learning objective is needed to map leaf-MCR to the appropriate position in the base-MCR space. To this end, we propose to learn the alignment densely among the quadruple semantic consistent pairs described in Sec. 3.2.1. In the case of the CLAP and CLIP, the dense inter-MCR alignment objectives are defined as:

$$\begin{aligned} L_{avc} &= \text{InfoNCE}(\hat{\mathbf{a}}^A, \tilde{\mathbf{v}}^I); & L_{tvc} &= \text{InfoNCE}(\hat{\mathbf{t}}^A, \tilde{\mathbf{v}}^I) \\ L_{atc} &= \text{InfoNCE}(\hat{\mathbf{a}}^A, \tilde{\mathbf{t}}^I); & L_{ttc} &= \text{InfoNCE}(\hat{\mathbf{t}}^A, \tilde{\mathbf{t}}^I) \end{aligned} \quad (5)$$

where the $\text{InfoNCE}(\cdot, \cdot)$ is the standard InfoNCE loss, which is defined as:

$$\text{InfoNCE}(\mathbf{x}, \mathbf{z}) = -\frac{1}{2} \frac{1}{N} \sum_{i=1}^N \left[\log \frac{\exp(\text{sim}(\mathbf{x}_i, \mathbf{z}_i)/\tau_2)}{\sum_{j=1}^N \exp(\text{sim}(\mathbf{x}_i, \mathbf{z}_j)/\tau_2)} + \log \frac{\exp(\text{sim}(\mathbf{z}_i, \mathbf{x}_i)/\tau_2)}{\sum_{j=1}^N \exp(\text{sim}(\mathbf{z}_i, \mathbf{x}_j)/\tau_2)} \right] \quad (6)$$

where the τ_2 is the temperature parameter. The overall loss for extending CLAP to CLIP is defined as a weighted combination of the intra-MCR and inter-MCR losses:

$$L = \lambda L_{intra} + \frac{1}{4} (L_{avc} + L_{atc} + L_{tvc} + L_{ttc}) \quad (7)$$

where λ is the hyper-parameter to balance the two terms.

For ULIP and CLIP, symmetric various modality-centric data 3.2.1, decoupled projector 3.2.2, and dense alignment loss 3.2.3 are employed to extend the 3D-image space to image-text space via the overlapping image modality.

Finally, we can use a unified representation space learning from existing MCRs for inference. Considering audio, text, image, and 3D point cloud inputs, we use CLAP’s audio encoder, CLIP’s text and image encoder, and ULIP’s 3D encoder to extract the corresponding features $\mathbf{a}_i^A, \mathbf{t}_i^I, \mathbf{v}_i^I, \mathbf{p}_i^U$. And the $\mathbf{t}_i^I, \mathbf{v}_i^I, f_m^A(f_l^A(\mathbf{a}_i^A))$ and $f_m^U(f_l^U(\mathbf{p}_i^U))$ are the final audio-text-image-3D unified representation learned by Ex-MCR, where the $f_m^A(\cdot), f_l^A(\cdot); f_m^U(\cdot), f_l^U(\cdot)$ are the learned projectors of CLAP and ULIP respectively.

4 EXPERIMENT

4.1 EXPERIMENTAL SETTING

Datasets For a fair comparison, we use the same unimodal datasets to C-MCR (Wang et al., 2023b) for training, totaling 2.3M texts, 1.3M images, 1.8M audio, and 0.8M 3D point cloud. More details about training datasets are provided in the Appendix.

Implementation Details We employ pre-trained frozen CLIP ViT-B/32 (Radford et al., 2021), CLAP (Wu et al., 2023), and ULIP v2 (PointBERT version) (Xue et al., 2023b) models. The temperature τ_1 in Eq. 1 2 for embedding aggregation is set to 0.01 following Wang et al. (2023b), while the τ_2 in 6 for InfoNCE loss calculation is set to 0.05. The hyper-parameter λ in Eq. 7 is set to 0.1. Following Wang et al. (2023b), we also add Gaussian noise with a variance of 0.004 to the semantic consistent embeddings described in Sec. 3.2.1. The linear projector $f_l(\cdot)$ is a simple linear layer, and the MLP projector $f_m(\cdot)$ is a 2-layer MLP. We train our model with a batch size of 4096 for 36 epochs. We employ the AdamW optimizer with an initial learning rate of 1e-3 and a cosine learning rate decay strategy.

Table 1: Results of audio-visual-text experiments. The best results are **bolded**.

Method	Audio-Image						Audio-Text		Image-Text	
	FlickrNet		AVE		VGGSS		AudioCaps		COCO	
	mAP	R@5	mAP	R@5	mAP	R@5	mAP	R@5	mAP	R@5
CLAP	-	-	-	-	-	-	21.98	35.23	-	-
CLIP	-	-	-	-	-	-	-	-	44.57	57.62
AudioCLIP	3.81	4.91	2.33	2.65	3.10	3.94	2.23	2.68	20.14	27.42
WAV2CLIP	2.77	3.41	3.48	4.23	7.42	10.47	0.88	0.99	44.57	57.62
C-MCR	4.74	5.97	4.21	4.91	5.95	7.69	9.50	13.62	24.56	33.83
Ex-MCR	4.94	5.95	4.46	4.93	6.39	8.12	11.19	16.65	44.57	57.62

Table 2: Results of 3d-visual-text experiments.

Method	3D-Text			3D-Image			Image-Text		
	ModelNet40			Objaverse-LVIS			COCO		
	Acc@1	Acc@3	Acc@5	mAP	R@1	R@5	mAP	R@1	R@5
CLIP	-	-	-	-	-	-	44.57	32.58	57.62
ULIP	60.40	79.00	84.40	3.54	1.45	4.51	34.42	22.92	46.33
ULIP v2	73.06	86.39	91.50	11.41	6.00	15.63	34.42	22.92	46.33
C-MCR	64.90	87.00	92.80	3.84	1.36	4.80	24.23	14.34	33.19
Ex-MCR	66.53	87.88	93.60	6.23	2.54	8.25	44.57	32.58	57.62

4.2 AUDIO-VISUAL-TEXT EXPERIMENT

Downstream tasks. We employ zero-shot audio-image, audio-text, and image-text retrieval tasks to evaluate the audio-image-text representations of Ex-MCR by extending CLAP to CLIP. For audio-image retrieval, we conduct evaluations on Flickr-SoundNet (Senocak et al., 2018), VGGSS (Chen et al., 2021), and AVE (Tian et al., 2018) datasets. Due to their small dataset sizes, we utilize all their available data, comprising 5,000, 5,000, and 4,097 samples. For audio-text retrieval, we utilize the validation set from the AudioCaps (Kim et al., 2019) dataset, which includes 964 audio samples, and for each audio, we choose one corresponding caption for retrieval. Regarding image-text retrieval, we employ the validation set of COCO (Lin et al., 2014) dataset, consisting of 5,000 images, each accompanied by text captions. We randomly select one text annotation for each image as the ground truth. We calculate the cosine similarity between modalities in representation space and use mAP and Top-5 metrics for performance comparison.

Performance Comparison. Fig. 1 compares Ex-MCR with WAV2CLIP, AudioCLIP, and C-MCR. Notably, even without using audio-image paired data, Ex-MCR achieves significantly better performance over WAV2CLIP and AudioCLIP, which illustrates that Ex-MCR is a more effective representation learning method when high-quality data pairs are limited. Furthermore, compared to C-MCR, Ex-MCR not only attains better audio-image alignment but also inherits more audio-text alignment from CLAP, with fully preserved image-text modality alignment of CLIP, which demonstrates the overall superiority of Ex-MCR over C-MCR in establishing new spaces and maintaining original spaces. In summary, extending CLAP to CLIP with our Ex-MCR method derives state-of-the-art audio-image-text unified representations.

4.3 3D-VISUAL-TEXT RESULTS

Downstream tasks. To evaluate the performance of 3D-image-text space learned by extending ULIP to CLIP, we conduct a zero-shot 3D object classification task to assess the alignment between 3D and text. We also perform zero-shot 3D-image and image-text retrieval tasks to evaluate the alignment between 3D and image, as well as image and text. The zero-shot 3D object classification task is carried on the ModelNet40 (Wu et al., 2015) validation set, comprising 2468 sample pairs across 40 different classes. We embed the label into 64 prompt templates for each class, then extracted and averaged the features to obtain the corresponding text embeddings, following Xue et al. (2023b). Regarding the zero-shot 3D-image retrieval task, we use the Objaverse-LVIS dataset (Deitke et al., 2023), which includes 46,054 3D objects. For each 3D object, ULIP v2 pro-

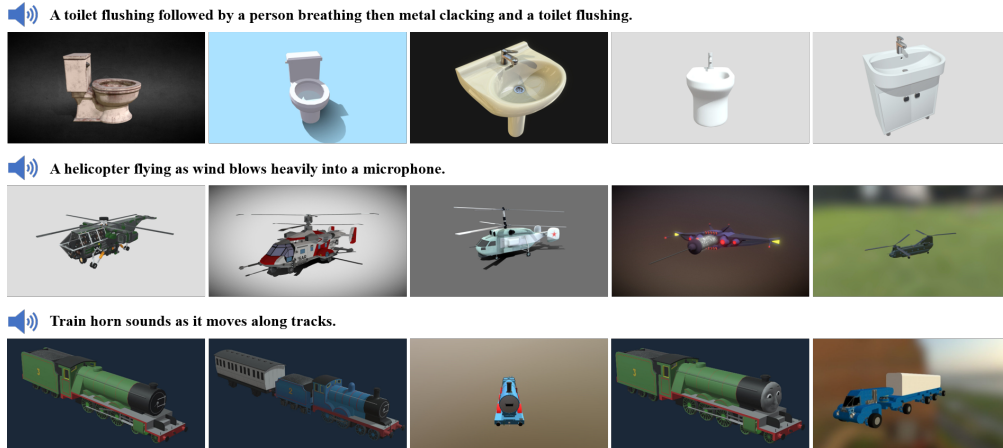


Figure 2: Visualization of Audio to 3D retrieval.

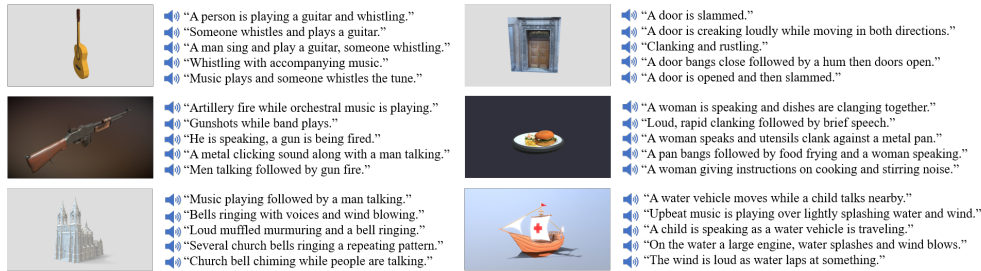


Figure 3: Visualization of 3D to Audio retrieval.

vides 12 rendered images from different perspectives, and we randomly selected one as the paired image. Additionally, we continued to use the COCO dataset’s validation set for zero-shot image-text retrieval.

Performance Comparison From Tab. 4.3, we can find the following key points. Firstly, even without using any 3D-text data, Ex-MCR still outperforms the advanced models (ULIP and ULIP v2) trained on 3D-text pairs in most performance metrics for 3D object classification. Secondly, the 3D-image retrieval accuracy of Ex-MCR is significantly higher than ULIP and C-MCR but lower than ULIP v2. Since the 3D-image space of ULIP v2 is treated as leaf-MCR, it is reasonable that Ex-MCR 3D-image performance is slightly lower than ULIP v2. At the same time, the better 3D-image retrieval accuracy than ULIP and C-MCR shows that Ex-MCR effectively learns strong 3D-image alignment. Finally, Ex-MCR retains the best image-text retrieval accuracy compared to these previous state-of-the-art models. The leading performance on all these tasks further demonstrates the superiority of Ex-MCR in unified contrastive representation learning.

4.4 EMERGENT 3D-AUDIO ALIGNMENT

In this section, we study whether the semantic alignment also emerges between the extended modalities (e.g., audio and 3D). We mutually retrieve audio in AudioCaps and 3D objects in Objaverse. In Fig. 2 and 3, we provide visualizations of some top-5 retrieval results, and audios are described by their corresponding caption annotations. These cases effectively demonstrate the emergent semantic alignment between audio-3D in Ex-MCR space. For example, the sound of a flushing toilet and water flow can retrieve 3D objects of toilets or sinks, while a sailboat 3D object can retrieve clips containing sounds of water vessels and wind. More results and the original audio files are provided in our supplementary material.

These exciting results demonstrate that extending ULIP and CLAP onto CLIP following our Ex-MCR methods derives a 3D-vision-text-audio unified contrastive representation space. In addition to the state-of-the-art performance on all possible tasks, Ex-MCR is an extremely training-efficient and paired-data-free representation learning method, which amplifies its application value in unified multi-modal representation learning.

4.5 ABLATION STUDIES

In this section, we analyze the main components of Ex-MCR. All experiments are conducted on extending CLAP to CLIP, and we reported the average mAP of audio-visual and audio-text retrieval on AVE and AudioCaps datasets, respectively. In addition, we also provide results on more datasets and evaluation metrics in the Appendix.

Table 3: Data modality-centric. A, I, and T represent audio-centric, image-centric, and text-centric data, respectively.

	AVE	AudioCaps
A	4.10	11.11
I	3.41	5.54
T	4.17	9.89
A+I	4.11	11.09
A+T	4.12	10.88
I+T	4.05	8.39
A+I+T	4.46	11.19

Table 4: Alignment objective. A-T, T-T, A-V, and T-V represent the alignment objective between audio-text, text-text, audio-image, and text-image, respectively.

	AVE	AudioCaps
A-T	4.00	10.82
T-T	4.15	11.30
A-V	3.97	7.49
T-V	4.18	7.68
All	4.46	11.19

Table 5: Structure of $f_1(\cdot)$

$f_1(\cdot)$	AVE	AudioCaps
Linear	4.46	11.19
1 MLP	4.16	10.25
2 MLP	4.04	9.93

Table 6: Structure of $f_m(\cdot)$

$f_m(\cdot)$	AVE	AudioCaps
Linear	3.70	11.15
1 MLP	4.15	10.53
2 MLP	4.46	11.19
3 MLP	4.31	11.30
4 MLP	4.35	11.07
5 MLP	4.42	10.93

Various modality-centric data As described in Sec. 3.2.1, We employ various modality-centric data to train our projectors. For investigating the effect of different modality-centric data, we ablate each modality-centric data, and the results are reported in Tab. 3. Each kind of data is beneficial for audio-visual and audio-image alignment, and using all kinds of data simultaneously brings the best performance.

Dense alignment objective To analyze the impact of different alignment objectives, we train the model with each alignment objective. From the results reported in Tab. 4, we can find that aligning the overlapping modalities (text) is most important. In terms of audio-visual alignment, directly aligning the pseudo-audio-visual pairs shows sub-optimal performance, which proves that the pseudo-data aggregating process is biased and noisy, and the pseudo-audio-visual data pair is most severely affected by noise. On the other hand, for audio-text alignment, the model using text-text alignment objective surpasses that of directly aligning pseudo-audio-text pairs, which further demonstrates the importance of alignment learned from overlapping modality.

Structure of $f_l(\cdot)$ Tab. 5 demonstrates the impact of different structures of $f_l(\cdot)$. The results prove our hypothesis: the representation structures between different modalities within one MCR space are similar, and a simple linear layer is enough to bridge the modality gap. Moreover, MLP with an activation layer introduces non-linearity, which may disrupt the representation’s spatial structure, bringing sub-optimal performance.

Structure of $f_m(\cdot)$ The impact of structures of $f_m(\cdot)$ is summarized in Tab. 6. For aligning to distinct MCR space, the non-linear MLP structure is better than the simple linear layer. Besides, our experiments show that 2-layer MLP may be enough, and more layers would not bring further performance improvement.

5 CONCLUSION

This paper proposes **Extending Multi-modal Contrastive Representations (Ex-MCR)**, a novel training-efficient and paired-data-free unified contrastive representation learning method for more than three modalities. Ex-MCR effectively integrates the knowledge in pre-trained MCRs through overlapping modalities between these MCRs. By extending ULIP and CLAP onto CLIP via the

overlapping image and text modality, respectively, we derive unified and high-quality audio-image-text-3D representations. Without using any paired data, Ex-MCR attains a series of state-of-the-art performance results across various tasks. More importantly, semantic alignment is also observed between extended modalities (e.g., audio-3D), which highlights the potential of Ex-MCR in modality extensibility.

REFERENCES

- Panos Achlioptas, Ahmed Abdelreheem, Fei Xia, Mohamed Elhoseiny, and Leonidas Guibas. Referit3d: Neural listeners for fine-grained 3d object identification in real-world scenes. In *Computer Vision—ECCV 2020: 16th European Conference, Glasgow, UK, August 23–28, 2020, Proceedings, Part I 16*, pp. 422–440. Springer, 2020.
- Daichi Azuma, Taiki Miyanishi, Shuhei Kurita, and Motoaki Kawanabe. Scanqa: 3d question answering for spatial scene understanding. In *proceedings of the IEEE/CVF conference on computer vision and pattern recognition*, pp. 19129–19139, 2022.
- Angel X Chang, Thomas Funkhouser, Leonidas Guibas, Pat Hanrahan, Qixing Huang, Zimo Li, Silvio Savarese, Manolis Savva, Shuran Song, Hao Su, et al. Shapenet: An information-rich 3d model repository. *arXiv preprint arXiv:1512.03012*, 2015.
- Dave Zhenyu Chen, Angel X Chang, and Matthias Nießner. Scanrefer: 3d object localization in rgb-d scans using natural language. In *European conference on computer vision*, pp. 202–221. Springer, 2020a.
- Honglie Chen, Weidi Xie, Andrea Vedaldi, and Andrew Zisserman. Vggsound: A large-scale audio-visual dataset. In *ICASSP 2020-2020 IEEE International Conference on Acoustics, Speech and Signal Processing (ICASSP)*, pp. 721–725. IEEE, 2020b.
- Honglie Chen, Weidi Xie, Triantafyllos Afouras, Arsha Nagrani, Andrea Vedaldi, and Andrew Zisserman. Localizing visual sounds the hard way. In *Proceedings of the IEEE/CVF Conference on Computer Vision and Pattern Recognition*, pp. 16867–16876, 2021.
- Angela Dai, Angel X Chang, Manolis Savva, Maciej Halber, Thomas Funkhouser, and Matthias Nießner. Scannet: Richly-annotated 3d reconstructions of indoor scenes. In *Proceedings of the IEEE conference on computer vision and pattern recognition*, pp. 5828–5839, 2017.
- Matt Deitke, Dustin Schwenk, Jordi Salvador, Luca Weihs, Oscar Michel, Eli VanderBilt, Ludwig Schmidt, Kiana Ehsani, Aniruddha Kembhavi, and Ali Farhadi. Objaverse: A universe of annotated 3d objects. In *Proceedings of the IEEE/CVF Conference on Computer Vision and Pattern Recognition*, pp. 13142–13153, 2023.
- Benjamin Elizalde, Soham Deshmukh, Mahmoud Al Ismail, and Huaming Wang. Clap learning audio concepts from natural language supervision. In *ICASSP 2023-2023 IEEE International Conference on Acoustics, Speech and Signal Processing (ICASSP)*, pp. 1–5. IEEE, 2023.
- Oran Gafni, Adam Polyak, Oron Ashual, Shelly Sheynin, Devi Parikh, and Yaniv Taigman. Make-a-scene: Scene-based text-to-image generation with human priors. In *European Conference on Computer Vision*, pp. 89–106. Springer, 2022.
- Zhe Gan, Linjie Li, Chunyuan Li, Lijuan Wang, Zicheng Liu, Jianfeng Gao, et al. Vision-language pre-training: Basics, recent advances, and future trends. *Foundations and Trends® in Computer Graphics and Vision*, 14(3–4):163–352, 2022.
- Jort F Gemmeke, Daniel PW Ellis, Dylan Freedman, Aren Jansen, Wade Lawrence, R Channing Moore, Manoj Plakal, and Marvin Ritter. Audio set: An ontology and human-labeled dataset for audio events. In *2017 IEEE international conference on acoustics, speech and signal processing (ICASSP)*, pp. 776–780. IEEE, 2017.
- Rohit Girdhar, Alaeldin El-Nouby, Zhuang Liu, Mannat Singh, Kalyan Vasudev Alwala, Armand Joulin, and Ishan Misra. Imagebind: One embedding space to bind them all. In *Proceedings of the IEEE/CVF Conference on Computer Vision and Pattern Recognition*, pp. 15180–15190, 2023.

-
- Yuan Gong, Andrew Rouditchenko, Alexander H Liu, David Harwath, Leonid Karlinsky, Hilde Kuehne, and James R Glass. Contrastive audio-visual masked autoencoder. In *The Eleventh International Conference on Learning Representations*, 2022.
- Ziyu Guo, Renrui Zhang, Xiangyang Zhu, Yiwen Tang, Xianzheng Ma, Jiaming Han, Kexin Chen, Peng Gao, Xianzhi Li, Hongsheng Li, and Pheng-Ann Heng. Point-bind & point-llm: Aligning point cloud with multi-modality for 3d understanding, generation, and instruction following, 2023.
- Andrey Guzhov, Federico Raue, Jörn Hees, and Andreas Dengel. Audioclip: Extending clip to image, text and audio. In *ICASSP 2022-2022 IEEE International Conference on Acoustics, Speech and Signal Processing (ICASSP)*, pp. 976–980. IEEE, 2022.
- Jiaming Han, Renrui Zhang, Wenqi Shao, Peng Gao, Peng Xu, Han Xiao, Kaipeng Zhang, Chris Liu, Song Wen, Ziyu Guo, et al. Imagebind-llm: Multi-modality instruction tuning. *arXiv preprint arXiv:2309.03905*, 2023.
- Deepti Hegde, Jeya Maria Jose Valanarasu, and Vishal M Patel. Clip goes 3d: Leveraging prompt tuning for language grounded 3d recognition. *arXiv preprint arXiv:2303.11313*, 2023.
- Rongjie Huang, Jiawei Huang, Dongchao Yang, Yi Ren, Luping Liu, Mingze Li, Zhenhui Ye, Jinglin Liu, Xiang Yin, and Zhou Zhao. Make-an-audio: Text-to-audio generation with prompt-enhanced diffusion models. *arXiv preprint arXiv:2301.12661*, 2023a.
- Shaohan Huang, Li Dong, Wenhui Wang, Yaru Hao, Saksham Singhal, Shuming Ma, Tengchao Lv, Lei Cui, Owais Khan Mohammed, Qiang Liu, et al. Language is not all you need: Aligning perception with language models. *arXiv preprint arXiv:2302.14045*, 2023b.
- Chao Jia, Yinfei Yang, Ye Xia, Yi-Ting Chen, Zarana Parekh, Hieu Pham, Quoc Le, Yun-Hsuan Sung, Zhen Li, and Tom Duerig. Scaling up visual and vision-language representation learning with noisy text supervision. In *International conference on machine learning*, pp. 4904–4916. PMLR, 2021.
- Chris Dongjoo Kim, Byeongchang Kim, Hyunmin Lee, and Gunhee Kim. Audiocaps: Generating captions for audios in the wild. In *Proceedings of the 2019 Conference of the North American Chapter of the Association for Computational Linguistics: Human Language Technologies, Volume 1 (Long and Short Papers)*, pp. 119–132, 2019.
- Junnan Li, Ramprasaath Selvaraju, Akhilesh Gotmare, Shafiq Joty, Caiming Xiong, and Steven Chu Hong Hoi. Align before fuse: Vision and language representation learning with momentum distillation. *Advances in neural information processing systems*, 34:9694–9705, 2021.
- Junnan Li, Dongxu Li, Caiming Xiong, and Steven Hoi. Blip: Bootstrapping language-image pre-training for unified vision-language understanding and generation. In *International Conference on Machine Learning*, pp. 12888–12900. PMLR, 2022.
- Weixin Liang, Yuhui Zhang, Yongchan Kwon, Serena Yeung, and James Zou. Mind the gap: Understanding the modality gap in multi-modal contrastive representation learning, 2022.
- Chen-Hsuan Lin, Jun Gao, Luming Tang, Towaki Takikawa, Xiaohui Zeng, Xun Huang, Karsten Kreis, Sanja Fidler, Ming-Yu Liu, and Tsung-Yi Lin. Magic3d: High-resolution text-to-3d content creation. In *Proceedings of the IEEE/CVF Conference on Computer Vision and Pattern Recognition*, pp. 300–309, 2023a.
- Tsung-Yi Lin, Michael Maire, Serge Belongie, James Hays, Pietro Perona, Deva Ramanan, Piotr Dollár, and C Lawrence Zitnick. Microsoft coco: Common objects in context. In *Computer Vision—ECCV 2014: 13th European Conference, Zurich, Switzerland, September 6–12, 2014, Proceedings, Part V 13*, pp. 740–755. Springer, 2014.
- Yan-Bo Lin, Yi-Lin Sung, Jie Lei, Mohit Bansal, and Gedas Bertasius. Vision transformers are parameter-efficient audio-visual learners. In *Proceedings of the IEEE/CVF Conference on Computer Vision and Pattern Recognition*, pp. 2299–2309, 2023b.

-
- Haohe Liu, Qiao Tian, Yi Yuan, Xubo Liu, Xinhao Mei, Qiuqiang Kong, Yuping Wang, Wenwu Wang, Yuxuan Wang, and Mark D Plumbley. Audioldm 2: Learning holistic audio generation with self-supervised pretraining. *arXiv preprint arXiv:2308.05734*, 2023a.
- Minghua Liu, Ruoxi Shi, Kaiming Kuang, Yinhao Zhu, Xuanlin Li, Shizhong Han, Hong Cai, Fatih Porikli, and Hao Su. Openshape: Scaling up 3d shape representation towards open-world understanding. *arXiv preprint arXiv:2305.10764*, 2023b.
- Shentong Mo and Pedro Morgado. A closer look at weakly-supervised audio-visual source localization. *Advances in Neural Information Processing Systems*, 35:37524–37536, 2022.
- Zhiliang Peng, Wenhui Wang, Li Dong, Yaru Hao, Shaohan Huang, Shuming Ma, and Furu Wei. Kosmos-2: Grounding multimodal large language models to the world. *arXiv preprint arXiv:2306.14824*, 2023.
- Ben Poole, Ajay Jain, Jonathan T Barron, and Ben Mildenhall. Dreamfusion: Text-to-3d using 2d diffusion. *arXiv preprint arXiv:2209.14988*, 2022.
- Alec Radford, Jong Wook Kim, Chris Hallacy, Aditya Ramesh, Gabriel Goh, Sandhini Agarwal, Girish Sastry, Amanda Askell, Pamela Mishkin, Jack Clark, et al. Learning transferable visual models from natural language supervision. In *International conference on machine learning*, pp. 8748–8763. PMLR, 2021.
- Aditya Ramesh, Prafulla Dhariwal, Alex Nichol, Casey Chu, and Mark Chen. Hierarchical text-conditional image generation with clip latents. *arXiv preprint arXiv:2204.06125*, 1(2):3, 2022.
- Robin Rombach, Andreas Blattmann, Dominik Lorenz, Patrick Esser, and Björn Ommer. High-resolution image synthesis with latent diffusion models. In *Proceedings of the IEEE/CVF conference on computer vision and pattern recognition*, pp. 10684–10695, 2022.
- Ludan Ruan, Yiyang Ma, Huan Yang, Huiguo He, Bei Liu, Jianlong Fu, Nicholas Jing Yuan, Qin Jin, and Baining Guo. Mm-diffusion: Learning multi-modal diffusion models for joint audio and video generation. In *Proceedings of the IEEE/CVF Conference on Computer Vision and Pattern Recognition*, pp. 10219–10228, 2023.
- Arda Senocak, Tae-Hyun Oh, Junsik Kim, Ming-Hsuan Yang, and In So Kweon. Learning to localize sound source in visual scenes. In *Proceedings of the IEEE Conference on Computer Vision and Pattern Recognition*, pp. 4358–4366, 2018.
- Yixuan Su, Tian Lan, Huayang Li, Jialu Xu, Yan Wang, and Deng Cai. Pandagpt: One model to instruction-follow them all. *arXiv preprint arXiv:2305.16355*, 2023.
- Zineng Tang, Ziyi Yang, Chenguang Zhu, Michael Zeng, and Mohit Bansal. Any-to-any generation via composable diffusion, 2023.
- Yapeng Tian, Jing Shi, Bochen Li, Zhiyao Duan, and Chenliang Xu. Audio-visual event localization in unconstrained videos. In *Proceedings of the European conference on computer vision (ECCV)*, pp. 247–263, 2018.
- Zehan Wang, Haifeng Huang, Yang Zhao, Ziang Zhang, and Zhou Zhao. Chat-3d: Data-efficiently tuning large language model for universal dialogue of 3d scenes. *arXiv preprint arXiv:2308.08769*, 2023a.
- Zehan Wang, Yang Zhao, Xize Cheng, Haifeng Huang, Jiageng Liu, Li Tang, Linjun Li, Yongqi Wang, Aoxiong Yin, Ziang Zhang, et al. Connecting multi-modal contrastive representations. *arXiv preprint arXiv:2305.14381*, 2023b.
- Ho-Hsiang Wu, Prem Seetharaman, Kundan Kumar, and Juan Pablo Bello. Wav2clip: Learning robust audio representations from clip. In *ICASSP 2022-2022 IEEE International Conference on Acoustics, Speech and Signal Processing (ICASSP)*, pp. 4563–4567. IEEE, 2022.
- Yusong Wu, Ke Chen, Tianyu Zhang, Yuchen Hui, Taylor Berg-Kirkpatrick, and Shlomo Dubnov. Large-scale contrastive language-audio pretraining with feature fusion and keyword-to-caption augmentation. In *ICASSP 2023-2023 IEEE International Conference on Acoustics, Speech and Signal Processing (ICASSP)*, pp. 1–5. IEEE, 2023.

-
- Zhirong Wu, Shuran Song, Aditya Khosla, Fisher Yu, Linguang Zhang, Xiaoou Tang, and Jianxiong Xiao. 3d shapenets: A deep representation for volumetric shapes. In *Proceedings of the IEEE conference on computer vision and pattern recognition*, pp. 1912–1920, 2015.
- Hu Xu, Gargi Ghosh, Po-Yao Huang, Dmytro Okhonko, Armen Aghajanyan, Florian Metze, Luke Zettlemoyer, and Christoph Feichtenhofer. Videoclip: Contrastive pre-training for zero-shot video-text understanding. *arXiv preprint arXiv:2109.14084*, 2021.
- Le Xue, Mingfei Gao, Chen Xing, Roberto Martín-Martín, Jiajun Wu, Caiming Xiong, Ran Xu, Juan Carlos Niebles, and Silvio Savarese. Ulip: Learning a unified representation of language, images, and point clouds for 3d understanding. In *Proceedings of the IEEE/CVF Conference on Computer Vision and Pattern Recognition*, pp. 1179–1189, 2023a.
- Le Xue, Ning Yu, Shu Zhang, Junnan Li, Roberto Martín-Martín, Jiajun Wu, Caiming Xiong, Ran Xu, Juan Carlos Niebles, and Silvio Savarese. Ulip-2: Towards scalable multimodal pre-training for 3d understanding. *arXiv preprint arXiv:2305.08275*, 2023b.
- Hang Zhang, Xin Li, and Lidong Bing. Video-llama: An instruction-tuned audio-visual language model for video understanding. *arXiv preprint arXiv:2306.02858*, 2023.
- Hang Zhao, Chuang Gan, Andrew Rouditchenko, Carl Vondrick, Josh McDermott, and Antonio Torralba. The sound of pixels. In *Proceedings of the European conference on computer vision (ECCV)*, pp. 570–586, 2018.
- Lichen Zhao, Daigang Cai, Lu Sheng, and Dong Xu. 3dvg-transformer: Relation modeling for visual grounding on point clouds. In *Proceedings of the IEEE/CVF International Conference on Computer Vision*, pp. 2928–2937, 2021.
- Yang Zhao, Zhijie Lin, Daquan Zhou, Zilong Huang, Jiashi Feng, and Bingyi Kang. Bubogpt: Enabling visual grounding in multi-modal llms. *arXiv preprint arXiv:2307.08581*, 2023.

A TRAINING DATASET

The details of our training dataset, which are mentioned in Sec. 4.1, are shown below.

Text Dataset. To ensure that the texts contain sufficient information for other modalities, the data of text is sourced from diverse perspectives in vision-text datasets (COCO, CC3M), video-text datasets (MSRVTT, MAD), and audio-text datasets (AudioCaps, Clotho). Following Wang et al. (2023b), we select 1M texts from CC3M. There are 2.33M text samples in total. We extract their CLAP and CLIP features \mathbf{T}^A and \mathbf{T}^I using the CLAP and CLIP encoders, respectively.

Image Dataset. For another modality in base-MCR, Vision, we utilize ImageNet1K as the data source. ImageNet1K is a large-scale image recognition dataset consisting of 1.3 million images. We extract their features to the sets \mathbf{V}^I , and \mathbf{V}^U in CLIP and ULIP, using the CLIP Encoder and ULIP Encoder.

Audio Dataset. AudioSet is a large-scale audio dataset with 2.1M audio clips from YouTube, equivalent to 5.8 thousand hours of audio and encompassing over 500 sound classes. We use the CLAP audio encoder to extract the feature set \mathbf{A}^A from the audios of the training set.

3D Point Cloud Dataset. For the 3D modality, we use Objaverse, the recently released and large-scale 3D objects dataset. It has approximately 800K real-world 3D objects. All 3D data are transformed into point clouds and extracted into the feature set \mathbf{P}^U using the ULIP 3D encoder.

It is worth noting that we do not employ any annotations provided with the datasets mentioned above as part of our training data, which means we only use the unimodal modality of data in each dataset we selected.

B ARCHITECTURE OF PROJECTORS

Table 7: Model configurations of projectors.

Module	Block	C_{in}	C_{out}
$f_1(\cdot)$	Linear	512	512
$f_m(\cdot)$	Linear	512	1024
	BatchNorm1D	1024	1024
	Relu	-	-
	Linear	1024	512
	BatchNorm1D	512	512
	Relu	-	-
	Linear	512	1024
	BatchNorm1D	1024	1024
	Relu	-	-
	Linear	1024	512
	BatchNorm1D	512	512
	Relu	-	-

The model configurations of our projectors are shown in Tab. 7.

C DETAILED RESULTS OF ABLATION STUDY

As a supplement to Tab. 3, Tab. 4, Tab. 5, and Tab. 6, we provide detailed ablation experiment results on more comprehensive evaluation metrics of various datasets, as shown below.

Table 8: Detailed results of experiments on data modality-centric.

Data Perspective	FlickrNet		AVE		VGGSS		AudioCaps	
	mAP	R@5	mAP	R@5	mAP	R@5	mAP	R@5
A	3.94	4.77	4.10	4.66	5.47	6.95	11.11	16.39
I	3.83	4.63	3.41	3.70	4.82	5.96	5.54	7.18
T	4.85	5.96	4.17	4.61	5.72	7.23	9.89	14.47
A+I	4.22	4.96	4.11	4.71	6.01	7.78	11.09	16.91
A+T	4.63	5.56	4.12	4.64	5.88	7.57	10.88	16.23
I+T	4.70	5.82	4.05	4.34	5.84	7.36	8.39	12.09
A+I+T	4.94	5.95	4.46	4.93	6.39	8.12	11.19	16.65

Table 9: Detailed results of experiments on the structure of $f_1(\cdot)$.

$f_1(\cdot)$	FlickrNet		AVE		VGGSS		AudioCaps	
	mAP	R@5	mAP	R@5	mAP	R@5	mAP	R@5
Linear	4.94	5.95	4.46	4.93	6.39	8.12	11.19	16.65
1 MLP	4.54	5.59	4.16	4.75	6.50	8.54	10.25	14.92
2 MLP	4.36	5.15	4.04	4.66	6.00	7.63	9.93	14.48

Table 10: Detailed results of experiments on the structure of $f_m(\cdot)$.

$f_m(\cdot)$	FlickrNet		AVE		VGGSS		AudioCaps	
	mAP	R@5	mAP	R@5	mAP	R@5	mAP	R@5
Linear	3.62	4.50	3.70	4.03	5.40	6.82	11.15	16.37
1 MLP	4.62	5.79	4.15	4.76	5.81	7.28	10.53	15.87
2 MLP	4.94	5.95	4.46	4.93	6.39	8.12	11.19	16.65
3 MLP	4.85	5.93	4.31	4.88	6.57	8.70	11.30	17.10
4 MLP	4.95	6.20	4.35	4.84	6.55	8.57	11.07	16.23
5 MLP	4.79	6.02	4.42	5.15	6.59	8.63	10.93	16.21

Table 11: Detailed results of experiments on alignment objective.

Objective	FlickrNet		AVE		VGGSS		AudioCaps	
	mAP	R@5	mAP	R@5	mAP	R@5	mAP	R@5
A-T	4.01	4.78	4.00	4.56	5.70	7.28	10.82	15.87
T-T	4.56	5.33	4.15	4.54	5.68	6.86	11.30	16.93
A-V	4.30	5.34	3.97	4.51	5.91	7.30	7.49	10.35
T-V	4.77	6.03	4.18	4.92	5.43	6.93	7.68	10.36
Dense	4.94	5.95	4.46	4.93	6.39	8.12	11.19	16.65